

Preparation and Characterization of a Dispersion Toughened Ceramic for Thermomechanical Uses (ZTA). Part II: Thermomechanical Characterization. Effect of Microstructure and Temperature on Toughening Mechanisms

G. Orange, G. Fantozzi

GEMPPM (CRRACS), URA 341, INSA, Bât. 502, F 69621 Villeurbanne Cedex, France

P. Homerin, F. Thevenot

ENSMSE (CRRACS), 158, Cours Fauriel, F 42023 Saint Etienne, France

&

A. Leriche, F. Cambier

CRIBC, 4. Av. Gouverneur Cornez, B 7000 Mons, Belgium

(Received 23 November 1990; revised version received 14 August 1991; accepted 15 August 1991)

Abstract

According to the composition and processing conditions, different microstructures of zirconia toughened alumina (ZTA) materials can be obtained (as shown in Part I of this paper). The mechanical behavior of the different ZTA materials was determined at room and high temperatures: fracture strength and toughness (σ_f , K_{IC}), slow crack growth resistance ($K_1 - v$). Zirconia toughened alumina composites present improved fracture properties compared to pure alumina. Thermal fatigue resistance is also improved compared to pure Al_2O_3 or ZrO_2 (Y-TZP) materials. The decrease of hardness by increasing addition of ZrO_2 particles is counterbalanced in part by toughening effects and the wear resistance can be improved for some compositions.

Two predominant and interacting toughening mechanisms are operative at low temperature: stress-induced phase transformation toughening (TT) and microcracking toughening (MT). Both toughening mechanisms are temperature dependent, but at different rates. The toughening and strengthening effects are discussed on the basis of transformation of

metastable zirconia particles depending on ZrO_2 and stabilizing agent (Y_2O_3) contents, on the particle size and on the temperature.

Infolge der unterschiedlichen Zusammensetzungen und Herstellungsbedingungen, konnten für ZTA-Werkstoffe unterschiedliche Mikrostrukturen realisiert werden (vgl. Teil I). Das mechanische Verhalten der verschiedenen, verstärkten ZTA-Werkstoffe wurde in Abhängigkeit von der Temperatur ermittelt: Bruchfestigkeit und Bruchzähigkeit (σ_f , K_{IC}) und unterkritisches Rißwachstum ($K_1 - v$). Die Verbundwerkstoffe Aluminiumoxid-Zirkonoxid zeigen deutlich verbesserte Brucheigenschaften gegenüber denen eines reinen Aluminiumoxids. Der thermische Bruchwiderstand ist gleichfalls, im Vergleich zum reinen Aluminiumoxid oder zum Zirkonoxid (Y-TZP), verbessert. Der bei steigendem Zirkonoxidanteil beobachtete Härteabfall wird zum Teil durch die Verstärkungseffekte ausgeglichen und der Verschleißwiderstand bei einigen Verbundwerkstoffen erhöht.

Bei niederen Temperaturen sind zwei sich gegenseitig beeinflussende Verstärkungsmechanismen vor-

herrschend wirksam: Die spannungsinduzierte Phasenumwandlung und die Mikrorißverstärkung. Beide sind jedoch in unterschiedlichem Maße temperaturabhängig. Die Verstärkungseffekte werden vor dem Hintergrund der Umwandlung metastabiler ZrO_2 -Partikel in Abhängigkeit des ZrO_2 -Gehalts und den stabilisierenden Zusätzen (Y_2O_3), der Partikelgröße und der Temperatur diskutiert.

Selon les conditions de préparation et la composition, différentes microstructures d'alumines renforcées par des particules d'alumine (ZTA) ont été obtenues (cf. Part I). Le comportement mécanique de différentes alumines renforcées a été déterminé en fonction de la température: résistance à la rupture et ténacité (σ_f , K_{Ic}) croissance sous critique ($K_1 - v$). Les composites alumine-zircone présentent des propriétés nettement supérieures à celles de l'alumine. La résistance à la fatigue thermique est également améliorée par rapport à l'alumine ou à la zircone (Y-TZP). La décroissance de la dureté par l'addition de particules de zircone est partiellement contrebalancée par les effets de renforcement et ainsi la résistance à l'usure peut être améliorée pour certaines compositions.

Deux mécanismes de renforcement prédominent à basse température: le changement de phase induit par la contrainte (TT) et le mécanisme de microfissuration (MT). Les deux mécanismes dépendent de la température mais de manière sensiblement différente. Les effets de renforcement sont discutés sur la base de la transformation de particules de zircone métastables, cette transformation dépendant de la teneur en zircone et en stabilisant (Y_2O_3), de la taille des particules et de la température.

1 Introduction

Zirconia toughened alumina composites are of growing interest because of their interesting mechanical properties, particularly high fracture toughness. The different toughening mechanisms, e.g. stress-induced phase transformation toughening (TT), microcracking toughening (MT) and crack deflection toughening (CDT) have been separately analyzed from a theoretical point of view.¹ It is well recognized now that the predominant toughening mechanism depends on the alloy composition and microstructure: dilatational transformation toughening with shear modification in partially stabilized zirconia (PSZ), uniaxial transformation and microcrack mechanisms in zirconia toughened alumina (ZTA), and transformation toughening (with partial

reversibility) in tetragonal zirconia polycrystals (TZP).² Environmental conditions, such as temperature, loading rate, etc., are also determining parameters in controlling toughening mechanisms. So, it is important to observe the toughening effects for well-controlled compositions under different conditions (temperature, slow or catastrophic crack propagation) and to consider the effect of toughening not only in terms of increase of toughness and/or fracture strength but also the dependence of other mechanical properties on the ZrO_2 particles dispersion.

Extremely different results are reported in the literature about the mechanical behavior of ZTA composites, and especially the dependence on temperature or the thermal shock resistance. As a consequence, it is very difficult to compare the materials even at a controlled grain size or composition.

The different ZTA compositions prepared by different processing methods (see Part I) are characterized in this paper (Part II) from a mechanical point of view. The mechanical properties temperature dependence is observed on optimized materials, i.e. the materials obtained with a combined dispersion method. Other properties such as the slow crack growth resistance, the thermal fatigue and the wear behavior are also determined on some Al_2O_3 - ZrO_2 compositions and compared to Al_2O_3 or ZrO_2 (TZP) characteristics. These properties can be correlated to the microstructure and processing conditions, i.e. to the metastable zirconia particle transformation depending on ZrO_2 and Y_2O_3 contents, particle size and temperature.

2 Experimental Procedure

Fracture strength (σ_f), elastic modulus (E) and fracture toughness (K_{Ic}) were measured on carefully prepared specimens (diamond machining and polishing) by three-point bending on hot-pressed materials (specimen size: $18 \times 4 \times 3 \text{ mm}^3$; span = 15 mm), and by four-point bending on pressureless sintered samples (specimen size: $36 \times 6 \times 4 \text{ mm}^3$; span = $7 \times 24 \text{ mm}$). K_{Ic} values were calculated from the conventional single edge notched beam method (notch tip radius: $40 \mu\text{m}$; relative notch depth: $a/w = 0.4$) on as-notched or annealed (1200°C , 15 min in air) specimens. Fracture energy values (G_{Ic}) are calculated from the mechanical parameters at room temperature. High-temperature experiments were performed in air, up to 1200°C . All tests were made at a constant displacement rate of 0.1 mm/min .

The slow crack growth resistance of some compositions was studied, at room temperature, by the double-torsion test (specimen size: $40 \times 20 \times 3 \text{ mm}^3$) using the relaxation method: $K_1 - v$ diagram, static fatigue parameters ($v = AK_1^n$).³

The thermal fatigue behavior was observed by acquisition of acoustic emission signals of thermally fatigued circular disc-shaped specimens (diameter: 30 mm; thickness = 3–5 mm) between a hot zone (furnace) and a cooling zone (pulsed air): the cooling rate was about $10^\circ\text{C}/\text{sec}$.¹⁰ Number of events were measured as a function of number of cycles N or temperature difference ΔT ; so the thermal life time N_c for a given ΔT or the critical temperature difference ΔT_c can be determined.

Wear tests were conducted on a block-on-ring tribometer, by rotating a steel ring (100 C6) against plane ceramic specimens (sliding speed = 0.36 m/s ; applied load = 700 N). The wear volume, calculated from the width of the trace, is determined as a function of sliding distance. Tests were performed in water media at room temperature.⁵

3 Composites Obtained by Mechanical Dispersion and Electrochemical Repulsion

The measured mechanical properties of pressureless sintered (PS) and hot-pressed (HP) specimens obtained according to the two processing methods are listed in Table 1: both processing routes give composites with improved properties compared to pure alumina. Drying conditions used with the slip-casting process lead to specific defects, and so the quite large observed dispersion of σ_f values. However, extreme values of about 700 MPa were obtained on some specimens (PS materials): this forming technique has also potential interest but needs an optimization to avoid the presence of large defects. Hot-pressed specimens have better σ_f values than pressureless sintered ones: this is correlated to the highest density and smallest grain size, both effects leading to a smaller critical defect size. In the case of composites with pure zirconia, hot pressing reduces the ZrO_2 grain size growth and as a consequence increases the relative metastable (tetragonal) ZrO_2 content T_r (as shown in Part I).

In materials obtained by the mechanical homogenization method (pressing), the evolution of toughness is correlated to the milling time and the content of yttria-stabilized ZrO_2 : all the particles are in a tetragonal state ($T_r = 100\%$). The toughening effect due to a stress-induced phase transformation mechanism is not clearly evident. The content of

Table 1. Mechanical properties of sintered $\text{Al}_2\text{O}_3\text{-ZrO}_2$ composites obtained by mechanical dispersion and electrochemical repulsion

Composition	Milling time (h)	Pressureless sintering (PS)		Hot pressing (HP)	
		σ_f (MPa)	K_{Ic} ($\text{MPa}\sqrt{\text{m}}$)	σ_f (MPa)	K_{Ic} ($\text{MPa}\sqrt{\text{m}}$)
(a) Mechanical homogenization (pressing)					
A10Z3Y	4.5	342	4.36	915	4.02
A15Z3Y	2.25	488	4.53	612	4.34
A15Z3Y	4.5	452	4.68	850	4.37
A15Z3Y	9	448	4.84	920	4.35
A15Z3Y	18	395	5.18	955	4.52
A20Z3Y	4.5	460	5.05	965	5.98
A45Z3Y	4.5	655	5.82	1200	8.72
(b) Electrochemical repulsion (slip casting)					
A5Z		575	4.6	759	5.27
A10Z		486	4.8	764	7.45
A15Z		433	4.7	773	5.65
A10Z1Y		507	5.9	788	5.55
A10Z2Y		331	5.4	757	5.13
A10Z3Y		358	4.3	690	5.03
A15Z1Y		492	5.2	779	5.82
A15Z2Y		447	4.4	808	5.85
A15Z3Y		632	4.5	915	5.42

stabilizing agent (Y_2O_3) seems to be quite high, except for the composition with 45 vol.% ZrO_2 : the critical stress for induced transformation is increased, and as a consequence the toughness increment (ΔK) is limited to low values. The milling time increases the fracture strength by a reduction of defect size: a milling time of 6 h seems to be an optimum. Longer milling times do not increase the toughness, and some contamination occurs (milling media).

In materials obtained by electrochemical repulsion, the effective toughening mechanism is a stress-induced phase transformation toughening at low ZrO_2 content with non-stabilized zirconia. Microcrack formation is enhanced as the ZrO_2 content is increased and as a consequence the strength values do not increase any further: an optimum is observed for 10 vol.% ZrO_2 in HP specimens, and 10 vol.% yttria-stabilized ZrO_2 (1 mol% Y_2O_3) in PS specimens. Addition of yttria-stabilized zirconia with higher contents are needed (20 vol.% yttria-stabilized zirconia and above) to observe significant toughening by stress-induced phase transformation; the same increase is observed with the fracture strength.

4 Composites Obtained by the Combined Dispersion Method

Mechanical milling gives a well-controlled grain size from the raw materials used, especially in reducing

Table 2. Mechanical properties of cast materials obtained by the combined dispersion method (slip-casting)

Composition	Pressureless sintering			Hot pressing		
	σ_f (MPa)	E (GPa)	K_{Ic} (MPa \sqrt{m})	σ_f (MPa)	E (GPa)	K_{Ic} (MPa \sqrt{m})
A5Z	382	370	5.7	672	388	5.51
A10Z	390	362	5.5	870	380	6.4
A15Z	370	348	4.90	485	360	4.15
A15Z1Y	330	344	6.1	470	365	6.35
A15Z2Y	415	345	5.6	1120	370	8.1
A15Z3Y	405	340	5.3	1140	366	7.3

the size of agglomerates, and the electrochemical repulsion leads to a good dispersion of the different phases. So, well-improved properties can be obtained by a combined process.

4.1 Materials obtained by slip-casting

The measured properties are listed in Table 2. Similar tendencies were observed as in the materials obtained by electrochemical repulsion (cf. Table 1, part (b)) except that all properties are well improved. This is a consequence of the combined mechanical milling process. Density values are quite high (\sim theoretical) even in PS materials.

Without stabilizing agent, σ_f and K_{Ic} values are improved with small additions of ZrO_2 (0–10 vol.%). In the case of PS materials, K_{Ic} values are nearly constant up to 10 vol.% ZrO_2 . There is no maximum of toughness (or of σ_f). For HP materials, K_{Ic} presents an optimum at 10 vol.% ZrO_2 . With Y_2O_3 (15 vol.% ZrO_2), the tetragonal phase is stabilized: there is no optimum of toughness in PS materials but an increase of σ_f values for Y_2O_3 content higher than 1 mol%. This is correlated to the diminution of monoclinic ZrO_2 content, and so the resultant

microcrack density. In HP materials, K_{Ic} is optimum at 2 mol% Y_2O_3 (15 vol.% ZrO_2): $K_{Ic} > 8$ MPa \sqrt{m} .

The toughening due to stress-induced phase transformation in ZTA materials is closely controlled by the residual stresses around confined particles: the increase of toughness (ΔK) is also greater as the density of the material is close to the theoretical density. This can explain in part the difference in behavior of PS and HP materials.

4.2 Materials obtained from spray-dried powders

The mechanical properties were determined at room temperature and also at high temperatures for some compositions. In Table 3, all the room temperature mechanical properties are listed: σ_f , K_{Ic} and the fracture energy (G_{Ic}). The dependence of mechanical properties on the ZrO_2 and Y_2O_3 contents is similar in these materials to that observed in the previous materials (slip-casted). But all properties are considerably increased with values of toughness of about 10.5 MPa \sqrt{m} (HP materials), and σ_f values as high as 1200 MPa (1650 MPa in as-machined specimens, without annealing treatment).

In PS materials, K_{Ic} values were nearly constant in

Table 3. Room temperature mechanical characteristics of materials obtained by the combined dispersion method from spray-dried powders (pressing)

Composition	Pressureless sintering			Hot pressing		
	σ_f (MPa)	K_{Ic} (MPa \sqrt{m})	G_{Ic} (Jm $^{-2}$)	σ_f (MPa)	K_{Ic} (MPa \sqrt{m})	G_{Ic} (Jm $^{-2}$)
A5Z	459	5.85	87	670	8.1	161
A10Z	412	6.25	105	735	9.25	214
A15Z	285	6.2	112	685	6.5	115
A20Z	75 (?)	5.75	130	625	6	129
A20Z1Y	480	5.6	85	830	8.2	178
A20Z2Y	558	6.5	120	(1118) ^a	10.9	315
					(10.1) ^a	(270) ^a
A20Z3Y	512	5.15	75	(1000) ^a	10.5	295
					(8.9) ^a	(212) ^a
A45Z3Y	675	11	385	1645	13.5	568
	(505) ^a	(7.8) ^a	(185) ^a	(1240) ^a	(10.65) ^a	(360) ^a

^a Annealing treatment (1200°C).

the range 5–15 vol.% ZrO_2 ($K_{Ic} = 6 \text{ MPa}\sqrt{\text{m}}$): no significant maximum is observed. σ_f values decrease drastically as the ZrO_2 content is increased above 10 vol.%. But for HP materials, a maximum of toughness values (K_{Ic}) is observed at 10 vol.% ZrO_2 ($K_{Ic} = 9.25 \text{ MPa}\sqrt{\text{m}}$) as also in the fracture strength (σ_f) between 5 and 15 vol.% ZrO_2 ($\sigma_f = 735 \text{ MPa}$). With yttrium zirconia, fracture properties (σ_f and K_{Ic}) increase with the volume fraction of metastable (tetragonal) particles in both PS and HP materials. The deviation between properties of as-machined and annealed specimens becomes more significant with high content of ZrO_2 (> 20 vol.%).

The fracture energy, G_{Ic} , corresponding to pure alumina, is about 40 J/m^2 . For 0–5 vol.% ZrO_2 in PS materials and up to 10 vol.% ZrO_2 in HP materials, the increase of G_{Ic} is mainly due to the contribution of a stress-induced phase transformation toughening mechanism (TT). Results are not completely consistent with the theoretical models of Evans & Cannon² or Lange,⁶ if a transformation zone size smaller than $10 \mu\text{m}$ is assumed for A10Z0Y (HP) material. In fact, a 'process zone' size of about $15\text{--}20 \mu\text{m}$ has to be introduced to obtain good agreement between experiments and theory. The 'process zone' values are higher than those reported by Kosmac *et al.*⁷ It is assumed in fact that TT is the only mechanism which contributes to the observed toughness. Other mechanisms have probably to be taken into account.

Above 15 vol.% ZrO_2 , the relative amount of tetragonal phase (T_r) is considerably reduced and microcracking toughening (MT) probably becomes the effective mechanism. This MT effect is not so energy dissipative as TT and the increase of G_{Ic} is limited (compared to pure alumina); similar G_{Ic} values (about 100 J/m^2) are observed in both HP and PS materials. Coupling effects between MT and TT are difficult to analyze and results cannot be compared to theoretical models.

With stabilizing agent additions, T_r increases: this is correlated with both the reduction of the mean ZrO_2 particle diameter, and the variation of the critical transformation diameter d_c (cf. Part I). Consequently, the stress-induced phase transformation toughening effect (TT) becomes more preponderant than microcracking toughening (MT), and G_{Ic} values increase. This evolution is observed on 20 vol.% ZrO_2 compositions with different amount of Y_2O_3 : there is an optimum for 2 mol% Y_2O_3 ($T_r = 100\%$). For higher Y_2O_3 content, the chemical free energy for the metastable transformation is reduced and therefore the fracture energy G_{Ic} decreases. The toughening effect is much

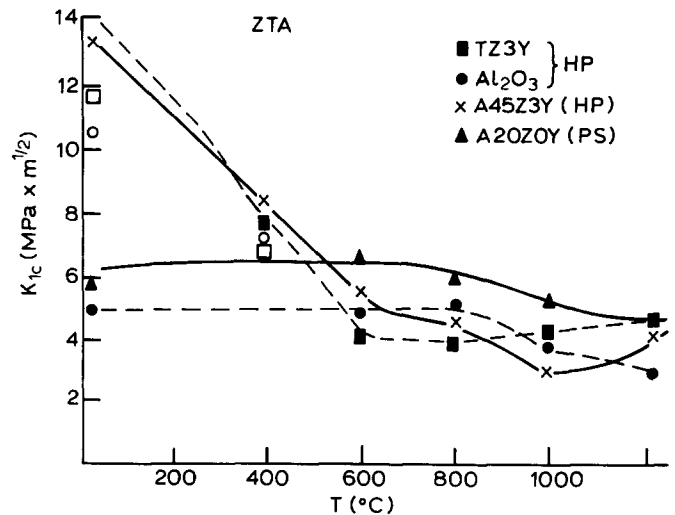


Fig. 1. Temperature dependence of fracture toughness of alumina, zirconia (TZP) and ZTA composites.

more pronounced as the proportion of transformable particles increases: the measured fracture energy is quite proportional to the amount of yttrium zirconia (up to 45 vol.% and above).

5 High Temperature Fracture Behavior of ZTA Composites

The temperature dependence of the mechanical properties ($\sigma_f(T)$, and $K_{Ic}(T)$) was observed for some PS and HP materials obtained according to the combined dispersion method (from spray-dried powders). Properties are reported in Figs 1 and 2. The authors have also reported measured values obtained for pure alumina and Y-TZP. For all tested ZTA composites, σ_f and K_{Ic} values decrease as temperature is increased. However, the K_{Ic} decreasing rate depends on the material composition and on the toughening mechanism of the considered

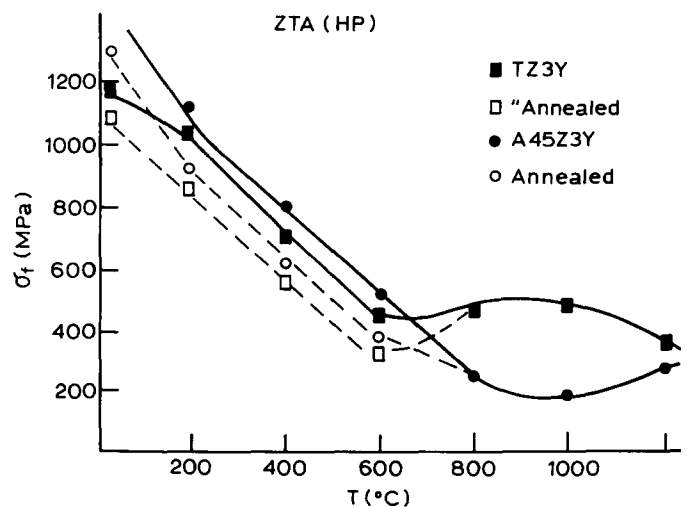


Fig. 2. Temperature dependence of fracture strength of zirconia (TZP) and ZTA composites.

material. Toughness values of pure alumina are quite constant up to 800°C, and decrease at higher temperatures. In contrast, Y-TZP materials exhibit very high values of strength and toughness at room temperature, but there is a drastic decrease in these values at higher temperatures (up to about 600°C). This temperature (600°C) corresponds to the critical temperature, T_0 , where transformation toughening is no more effective and the chemical free energy for transformation ΔG_c is equal to zero.⁸

For ZTA composites with 45 vol.% ZrO_2 (3 mol% Y_2O_3) where TT is the main toughening mechanism, a similar temperature dependence to that in Y-TZP is observed: properties are dramatically improved at room temperature but decrease drastically as the temperature is increased. However, the critical temperature T_0 is higher (about 700–800°C): this is explained by the higher elastic properties of the matrix (Al_2O_3).

Compositions with 20 vol.% ZrO_2 (without stabilizing additions), where MT is the preponderant toughening mechanism, present not so high properties at room temperature but they are quite temperature independent up to 800°C. This result supports the fact that microcracking toughening (MT) is not directly temperature dependent. Moreover, if the content of induced microcracks is high enough, some contribution to toughening by crack deflection or crack branching are possible and these mechanisms can be considered as temperature independent. At medium temperatures (500–600°C), these compositions in fact present a higher toughness than that of the strongest Y-TZP materials. At higher temperature (1000°C), the distribution of ZrO_2 particles avoid important plastic deformation. Some creep experiments support this observation.⁹

It is possible to explain the temperature dependence of toughness or fracture energy on temperature from the relation established by Becher *et al.*,¹⁰ or directly from the thermodynamic approach of Lange:⁶

$$K_c^2 = K_0^2 + \frac{2RE_c V_p (\Delta G_c - f\Delta U_d)}{1 - \nu_c^2} \quad (1)$$

where K_0 is the matrix toughness value, E_c , ν_c are the elastic constants of the composite, $\Delta G_c - f\Delta U_d$ is the work done, per unit volume, by the stress field to induce the phase transformation, and R is the size of the transformation zone. Some measured values are plotted in Fig. 3, and also some data from Lange's experiments are shown. Consistent results are obtained if it is assumed that the transformation zone size (R) is greater than the grain size (D): this is not in accordance with the Lange hypothesis.⁶

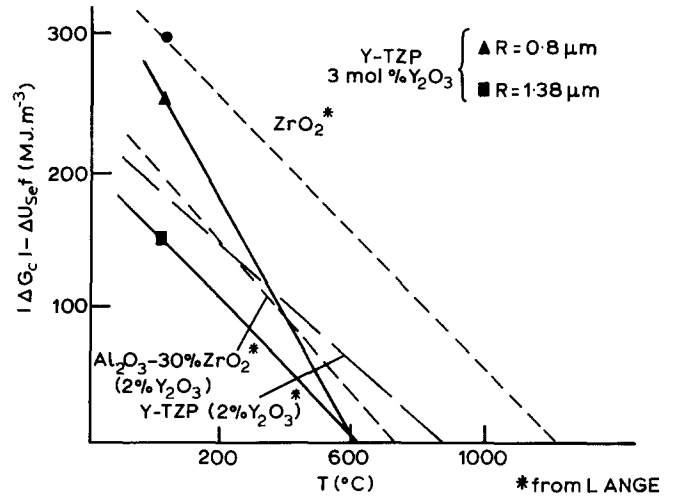


Fig. 3. Variation of the transformation energy, $\Delta G_c - f\Delta U_d$, as a function of temperature for TZP and different ZTA materials.

Moreover, the relative volume fraction of transformable tetragonal zirconia is about 30–45% (A45Z3Y, TZP). Calculated R values are larger in ZTA composites ($R = 10\text{--}15\ \mu\text{m}$, for 45 vol.% yttried ZrO_2) than in TZP materials ($R = 2\text{--}5\ \mu\text{m}$). This point is supported by the observed R -curve effect in these composite materials.^{11,12}

6 Effect of Dispersed Phase on some Mechanical Properties

6.1 Slow crack growth behavior

Different pressureless sintered compositions were processed so as to measure the static fatigue parameters: one composition was obtained by the mechanical homogenizing method with 15 vol.% yttried zirconia (A15Z3Y) and some compositions were obtained by the combined dispersion method (Al_2O_3 as a reference, A5Z, A20Z2Y). TZP specimens were also tested. The $(K_I - v)$ diagrams corresponding to TZP and ZTA composites are reported in Fig. 4. The slow crack growth parameters calculated from this diagram are presented in Table 4 with fracture properties (σ_f , K_{Ic}) of tested specimens.

Yttried zirconia composites (A15Z3Y) present similar σ_f and K_{Ic} values as alumina composites: this is due to the stabilization of the ZrO_2 tetragonal phase which does not transform any more in the stress field around main cracks. Nevertheless, static fatigue parameters are quite improved: n and A parameters (relation: $v = AK_I^n$), K_{I0} threshold stress where crack propagation is initiated.

This effect is confirmed by the observed dependence of the fracture strength (σ_f) on the strain rate ($\dot{\epsilon}$) during bending tests: ZTA composites processed by the combined dispersion method

Table 4. Mechanical properties and static fatigue parameters of ZTA composites

Composition	σ_r (MPa)	K_{Ic} (MPa \sqrt{m})	G_{Ic} (Jm $^{-2}$)	$K_{Ic, exp}$ (MPa \sqrt{m})	n	$\ln A$	A (m/s MPa \sqrt{m})
(a) Mechanically homogenized materials							
Alumina (RC 172)	310	4.4	49	4.1	37	565	
ZTA (C.S.) (A15Z3Y)	450	4.8	65	4.5	75	820	
(b) Materials obtained by the combined dispersion method and pressureless sintered							
RC172	270	4.55		5.1	72		10^{-97}
A5Z0Y	360	5.6		5.9	90		10^{-120}
A20Z2Y	425	5.95		5.5	80		10^{-73}
TZ3Y	802	9.6		7.6	80		10^{-145}

(pressureless sintering) with 10 vol.% ZrO₂ and 30 vol.% yttried ZrO₂ (2.5 mol% Y₂O₃) show respectively an n value of 45 and 75. Becher obtained similar results on a 20 vol.% ZrO₂ (3 mol% Y₂O₃) composite.¹³

From the double torsion test, a similar n parameter for alumina and tetragonal zirconia is observed, but the K_{10} threshold stress is higher in TZP material (with a lower value of A). Among the compositions obtained by the combined dispersion method, the ZTA composite with 5 vol.% ZrO₂ presents very much improved slow crack growth resistance (high n value and low A parameter). This characteristic is of fundamental implication for the use of such ceramic composites: a dispersion of ZrO₂ particles (stabilized or not) in Al₂O₃ matrix improves the slow crack growth resistance and as a consequence increases the reliability of large parts and the time to failure in service.

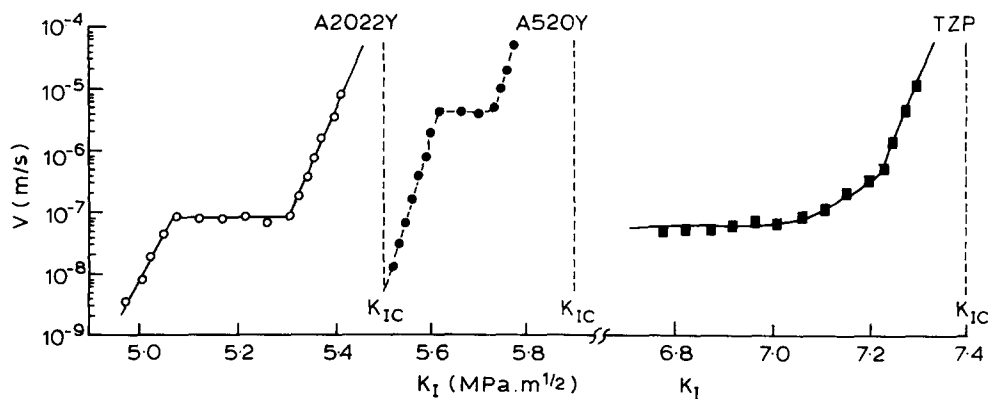
6.2 Thermal fatigue behavior

One composition (45 vol.% yttried ZrO₂-3 mol% Y₂O₃) obtained according to the mechanical homogenization method (pressureless sintering) was studied by thermal fatigue and compared to pure alumina and to Mg-PSZ or Y-TZP materials. The thermal lifetime N_c , defined as the number of cycles

to failure, is plotted for each temperature difference ΔT in Fig. 5. Thermal fatigue parameters (critical temperature difference ΔT_c , n' parameter (where $N_c (\Delta T)^{n'} = \text{Constant}$)) are reported in Table 5. The critical temperature ΔT_c , which corresponds to the specimen fracture at the first cycle ($N_c = 1$) is similar for TZP and ZTA materials. However, the slope (n') of $N_c - \Delta T$ curves is quite different: the n' parameter is a characteristic of the resistance to propagation of thermally induced cracks.¹⁴ If ZTA and Al₂O₃ materials are compared, n' parameters are similar, but ΔT_c values are different. The composites combine high values of ΔT_c with high resistance to thermally induced crack propagation. The good slow crack growth resistance of ZTA materials, as shown previously, can explain the improved thermal fatigue resistance of these materials, which can compete with alumina or zirconia ceramics for high-temperature applications.

Table 5. Thermal fatigue parameters

Composition	ΔT_c (°C)	n'
Al ₂ O ₃ (RC 172)	580	75
A45Z3Y	810	70
Mg-PSZ	740	100
Y-TZP	780	20

**Fig. 4.** ($K_I - v$) diagram of alumina, TZP and ZTA composites (log plot).

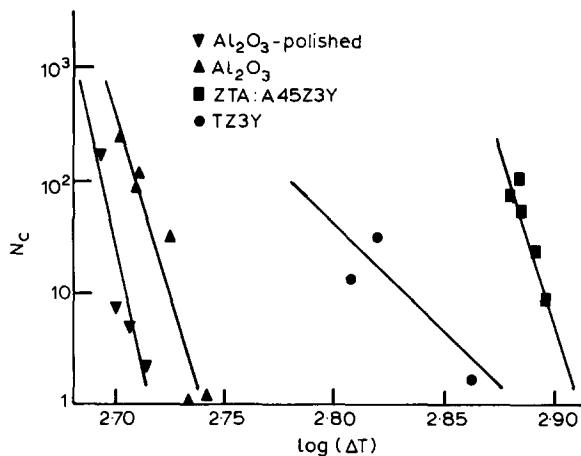


Fig. 5. Number of cycles to failure (N_c) as a function of temperature difference ΔT .

6.3 Wear behavior

The wear behavior has been characterized on ZTA compositions obtained with the combined dispersion method and densified by hot-pressing. The dispersion of ZrO_2 particles in Al_2O_3 matrix improves the fracture behavior but reduces the wear resistance: as the ZrO_2 content increases, the hardness and elastic modulus of the composites decrease. In the case of non-stabilized zirconia, the measured wear volume increases with the ZrO_2 volume fraction. Above 10 vol.% ZrO_2 , the phase transformation ($t \rightarrow m$) of particles produces microcracks which lead to a complete degradation of the sliding surface. The stabilization of ZrO_2 by addition of yttria reduces the wear volume. Figure 6 shows the variation of wear resistance for a high content of yttried zirconia (3 mol% Y_2O_3). Wear seems to be controlled by the two material properties, hardness and fracture toughness. A minimum of wear volume is observed at about 20–30 vol.% yttried ZrO_2 , because of toughening of the

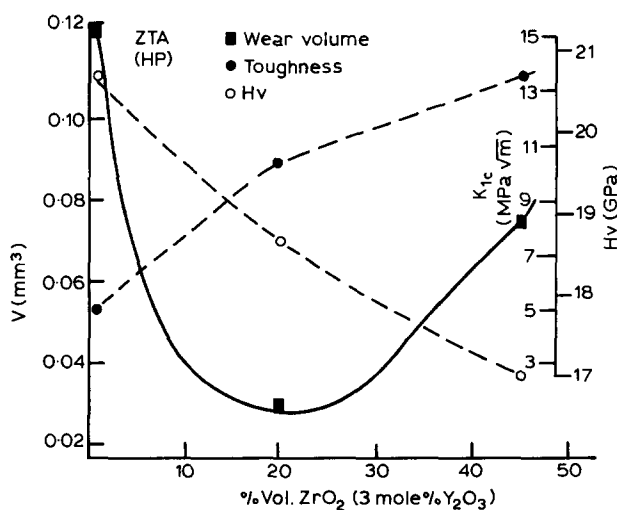


Fig. 6. Dependence of wear and fracture resistance on yttried ZrO_2 content.

specimen surfaces. Above 30 vol.% the decrease of elastic properties (elastic modulus and hardness) becomes more preponderant than the toughening of composites and a reduction in the wear resistance is observed. Zirconia toughened alumina composites can compete with the most successful zirconia materials.¹⁵

7 Conclusion

Zirconia toughened alumina (ZTA) composites were prepared from Al_2O_3 and ZrO_2 raw powders, using different fabrication processes (mechanical or electrochemical dispersion, pressureless sintering or hot pressing). Mechanical properties of the different Al_2O_3 - ZrO_2 materials are mainly much improved compared to pure alumina: not only σ_f and K_{Ic} but also the slow crack growth resistance and the thermal fatigue behavior. Different compositions were studied (low and high ZrO_2 content, with or without yttria); each of them has specific properties corresponding to the microstructure and the composition of the composite.

From the results, it can be noted that transformation toughening is effective in A5Z0Y (PS), A10Z0Y (HP), A20Z2Y (HP) and A45Z3Y (PS and HP). The size of the 'process zone' is about 10–20 μm (estimated from the experiments and theoretical models). For other compositions, multiple mechanisms are effective, and the analysis becomes very difficult.

The fracture behavior temperature dependence is much more pronounced as the toughening is obtained by phase transformation. Sub-critical crack growth is impeded by the presence of ZrO_2 particles. A good behavior is also observed with thermal fatigue and wear.

Acknowledgement

The authors are grateful to the EEC for financial support of part of this research (Contract numbers SUT 107 F, 110 F, 115 B).

References

1. Evans, A. G., Toughening mechanisms in zirconia alloy. *Science and Technology of Zirconia II, Advances in Ceramics*, Vol. 12, The American Ceramic Society USA, 1984, pp. 193–212.
2. Evans, A. G. & Cannon, R. N., Toughening of brittle solids by martensitic transformations. *Acta Met.*, **34**(5) (1986) 761–800.

3. Mamoun, A., Orange, G. & Fantozzi, G., Caractérisation de la propagation lente des fissures à hautes température par la méthode de double torsion. *Science of Ceramics*, **12** (1983) 557-62.
4. Busawon, M., Augustyniak, B., Fantozzi, G. & Rouby, D., Relation between acoustic emission and damage caused by thermal fatigue and thermal shocks in structural ceramics. In *2nd International Symposium on Ceramic Materials and Composites for Engines*, ed. W. Bunk & H. Hausner, 1986, pp. 799-806.
5. Trabelsi, R., Treheux, D., Orange, G., Fantozzi, G. & Thevenot, F., Relationship between mechanical properties and wear resistance of $\text{Al}_2\text{O}_3\text{-ZrO}_2$ ceramic composites. In *42nd Annual Meeting of the American Society of Lubrication Engineers*, Anaheim, CA, USA, May 1987.
6. Lange, F. F., Transformation toughening. *J. Mater. Sci.*, **17** (1982) Part 1, 225-34; Part 2, 235-9.
7. Kosmac, T., Swain, M. & Claussen, N., Role of tetragonal and monoclinic ZrO_2 particles in the fracture toughness of $\text{Al}_2\text{O}_3\text{-ZrO}_2$ composites. *Mat. Sci. Eng.*, **71** (1985) 57-64.
8. Orange, G. & Fantozzi, G., Mechanical properties and dependence with temperature of tetragonal polycrystalline zirconia materials. In *Fract. Mech. of Ceram.*, Vol. 7, ed. R. C. Bradt, A. G. Evans, D. P. H. Hasselman & F. F. Lange, Plenum Press, 1986, pp. 285-96.
9. Wakai, F., Iga, T., Nagano, T., Effect of dispersion of ZrO_2 particles on creep of fine-grained yttria-stabilized tetragonal zirconia. *Nippon Seramikkusu Kyokai Gakujutsu Ronbunshi*, **96**(12) (1988) 1206-9.
10. Becher, P. F., Swain, M. V. & Ferber, M. K., Relation of transformation temperature to the fracture toughness of transformation toughened ceramics. *J. Mater. Sci.*, **22** (1987) 76-84.
11. Steinbrech, R. W. & Heuer, A. H., R-Curve behaviour and mechanical properties of transformation-toughened ZrO_2 containing ceramics. In *Mater. Research Soc. Symposia*, Vol. 60, ed. Y. Chen, W. D. Kingery & R. J. Stokes, Material Research Society, Pittsburg, USA, 1986, pp. 369-81.
12. Saadaoui, M., Orange, G. & Fantozzi, G., Toughness and crack propagation resistance in transforming ceramic materials. In *1st European Ceram. Soc. Conf.*, Vol. 3, Maastricht, NL, June 89, pp. 155-9.
13. Becher, P. F., Slow crack growth behaviour in transformation-toughened $\text{Al}_2\text{O}_3\text{-ZrO}_2(\text{Y}_2\text{O}_3)$ ceramics. *J. Am. Ceram. Soc.*, **66**(7) (1983) 485-8.
14. Kamiya, N. & Kamigaito, N., Prediction of thermal fatigue life of ceramics. *J. Mater. Sci.*, **14** (1979) 573-82.
15. Fischer, T. E., Anderson, M. P. & Jahanmir, S., Influence of fracture toughness on the wear resistance of yttria-doped zirconium oxide. *J. Am. Ceram. Soc.*, **72**(2) (1989) 252-7.